### Title

fMRI of the rod scotoma elucidates cortical rod pathways and implications for lesion measurements




### Journal

Proceedings of the National Academy of Sciences of the United States of America, 112(16)

### ISSN

0027-8424



### Authors

Barton, Brian
Brewer, Alyssa A



### Publication Date

2015-04-21

### DOI

10.1073/pnas.1423673112

# fMRI of the rod scotoma elucidates cortical rod pathways and implications for lesion measurements

**Brian Barton[1] and Alyssa A. Brewer**

Department of Cognitive Sciences, University of California, Irvine, CA 92697

Edited by Brian A. Wandell, Stanford University, Stanford, CA, and approved March 16, 2015 (received for review December 10, 2014)

**Are silencing, ectopic shifts, and receptive field (RF) scaling in cortical scotoma projection zones (SPZs) the result of long-term reorganization (plasticity) or short-term adaptation? Electrophysiological studies of SPZs after retinal lesions in animal models remain controversial, because they are unable to conclusively answer this question because of limitations of the methodology. Here, we used functional MRI (fMRI) visual field mapping through population RF (pRF) modeling with moving bar stimuli under photopic and scotopic conditions to measure the effects of the rod scotoma in human early visual cortex. As a naturally occurring central scotoma, it has a large cortical representation, is free of traumatic lesion complications, is completely reversible, and has not reorganized under normal conditions (but can as seen in rod monochromats). We found that the pRFs overlapping the SPZ in V1, V2, V3, hV4, and VO-1 generally (*i*) reduced their blood oxygen level-dependent signal coherence and (*ii*) shifted their pRFs more eccentric but (*iii*) scaled their pRF sizes in variable ways. Thus, silencing, ectopic shifts, and pRF scaling in SPZs are not unique identifiers of cortical reorganization; rather, they can be the expected result of short-term adaptation. However, are there differences between rod and cone signals in V1, V2, V3, hV4, and VO-1? We did not find differences for all five maps in more peripheral eccentricities outside of rod scotoma influence in coherence, eccentricity representation, or pRF size. Thus, rod and cone signals seem to be processed similarly in cortex.**

functional MRI | scotopic | plasticity | adaptation | population receptive fields

A pressing question in visual neuroscience is, "To what extent can adult human visual cortex reorganize after the removal of visual input?" This question can be studied through the effects of retinal lesions (causing scotomas), in which input from the retina has been removed, but cortical representations of the scotoma projection zone (SPZ) remain intact. Accordingly, emphasis must be placed on teasing apart effects of scotomas that relate to short-term cortical adaptation from those of long-term cortical plasticity (1) (terminology review is in ref. 2). Here, we investigate this question in human cortex by using functional MRI (fMRI) to measure the immediate cortical SPZ responses in the unique paradigm of the naturally occurring rod scotoma.

The photoreceptors in humans can be divided into two classes: cones, which are primarily responsible for vision under high-luminance (photopic) conditions, and rods, which are primarily responsible for vision under low-luminance (scotopic) conditions when the cones are inactive. The cones are an order of magnitude more highly concentrated in the fovea relative to the periphery, where they inform our most detailed visual experience (3). In contrast, the greatest concentrations of rods are more than ∼10° eccentric from fixation and become increasingly sparse toward fixation until they are completely absent. This roughly circular rod-free zone covers a radius of ∼0.6–0.8° of visual angle about the fixation point (diameter = ∼1.25–1.7°) (4, 5). Under scotopic conditions, a scotoma arises from these foveal, rod-free zones, because no photoreceptors are stimulated within these regions (6, 7). Perceptual and fMRI estimates of the rod scotoma range from ∼1° to 2° of visual angle in radius because of the rod-sparse region surrounding the foveola and individual variability (6–9).

The properties of the rod scotoma make it an excellent candidate for studying the removal of visual input. First, the scotoma exists in all normal human subjects under scotopic conditions (5, 7). Second, the scotoma is located in the central fovea, which has large swaths of early visual cortex devoted to its analysis (10–12). Third, the scotoma arises because of the central fovea's complete lack and surrounding paucity of rod photoreceptors, allowing for a very close comparison with retinal lesions in animal models (5). Fourth, there is indirect evidence that the rod contributions to cortical activity are very similar to those of the cones, allowing for comparisons of changes in the properties of the cortical neurons overlapping the scotomas arising from either scotopic conditions or direct retinal lesions (6, 7, 13, 14). Fifth, the rod scotoma is completely reversible on return to photopic conditions, allowing for the measurement of ectopic cortical responses caused by short-term cortical adaptation without contamination from long-term reorganization, such as that seen in the relatively permanent developmental foveal scotomas of rod monochromats (7).

Keys to the use of the rod scotoma in the evaluation of cortical plasticity are the questions, "To what extent do the retinal differences between rod and cone photoreceptors influence cortical processing, and do any affects vary across cortical regions?" Rods have larger receptive fields (RFs) than cones and greater connectivity density with ganglion cells (4, 5), but do these differences survive center-surround mutual inhibitory networks to be measurably different at the cortical level (15, 16)? To answer all of these questions, the cortical effects of the rod scotoma must be differentiated from any effects caused by differences between rod and cone input.

To investigate the effects of the rod scotoma in human early visual cortex, we presently compared the retinotopic responses in

## Significance

We use functional MRI to investigate the cortical effects on V1, V2, V3, hV4, and VO-1 when humans' eyes have adapted to low-light vision. We show that populations of neurons with receptive fields interacting with the central rod scotoma are silenced because of lack of stimulation, shift their locations ectopically, and/or scale their sizes in some maps because of partial stimulation when the receptive fields overlap with the rod scotoma. These same effects have been cited as hallmarks of long-term reorganization, but our results show that these effects can be the result of the normal short-term adaptation of the visual system. In contrast, we observe no cortical differences between general rod and cone input other than rod scotoma effects.

Author contributions: B.B. and A.A.B. designed research, performed research, analyzed data, and wrote the paper.

The authors declare no conflict of interest.

This article is a PNAS Direct Submission.

[1]To whom correspondence should be addressed. Email: bbarton@uci.edu.

This article contains supporting information online at www.pnas.org/lookup/suppl/doi:10.1073/pnas.1423673112/-/DCSupplemental.



NEUROSCIENCE

early visual field maps V1, V2, V3, hV4, and VO-1 between photopic and scotopic conditions in normal adults. We expect three types of short-term adaptive responses from neurons in the SPZ of any scotoma in visual space. First, neurons with RFs completely eclipsed by the SPZ should be silenced, resulting in a reduction of neural activity to the spontaneous firing rate (Fig. 1*A*). At this population-level fMRI measurement, this effect will be reflected by a reduction in coherence. Second, neurons with RFs partially eclipsed by the SPZ should have an apparent ectopic shift of their preferred centers, because they will continue to respond to the remaining (now decreased) visual space. Such ectopic shifts occur whether the preferred center of that neuron is within the SPZ (Fig. 1*B*) or adjacent (Fig. 1*C*). Third, it is expected that neurons with RFs partially eclipsed by the SPZ may show a scaling of their RF sizes, although whether these increase or decrease in size is difficult to predict. Such neurons' new RF spans will necessarily be reduced by the overlap with the SPZ, but their RF sizes may also be increased because of changes in feedback activity or a reduction in lateral inhibitory connections to nearby neurons that have also been silenced or shifted to ectopic locations by the scotoma (1, 2, 17–20). The combination of these effects could also lead to no observable change at this level of measurement.

Each of these predicted scotoma effects must be distinguished from differences between photopic and scotopic conditions unrelated to the rod scotoma. The RFs of neurons in more peripheral eccentricities do not overlap with the rod scotoma, but they perform the same computations as their more central counterparts. As a result, they measure the effect of rod vs. cone inputs independent of the rod scotoma, acting as an ideal control with which the effects of the rod scotoma can be contrasted. First, because of the difference in luminance that defines photopic and scotopic conditions, we predict a reduction in coherence. Second, we predict no change in the locations of cortical RFs. Third, we test whether there is a change in RF size at the population level. The RFs of rods are larger than cones, and the retinal ganglion cells receive a greater number of inputs from rods than cones (4, 5), both of which suggest that we may observe larger cortical RFs. However, it is possible that, by the time that the signals reach cortex, center-surround mutual inhibition circuitry may counter any such increase in RF size, because the larger retinal RFs contribute to both the centers and surrounds of subcortical and cortical RFs (4, 5, 8, 13–16). Furthermore, any population of RFs in a cortical location, such as a voxel, will have a degree of dispersion of their preferred centers, which leads to a larger measured RF for the population as a whole relative to individual constituent RFs. As such, any change in RF size under scotopic relative to photopic conditions that survives center-surround mutual inhibitory networks may be indistinguishable from RF dispersion at the population level (17, 21, 22). Any differences in these measurements of coherence, preferred center, and size of populations of RFs caused by the rod scotoma in the central eccentricities must extend beyond any differences observed in more peripheral eccentricities caused by differences between photopic and scotopic conditions.

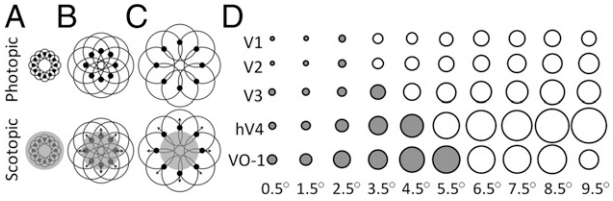


**Fig. 1.** Schematic of the predicted effects of the rod scotoma. (*A*–*C*) Black disks and black circles around them indicate the preferred center and spread of a neuron's RF, respectively. Each row, thus, represents neurons with preferred centers at one specific eccentricity. (*Lower*) The gray shaded regions indicate the SPZ of the rod scotoma under scotopic conditions. Black arrows indicate the expected direction of the measured shift of RF centers caused by interaction of the rod scotoma with a neuron's RF under scotopic relative to photopic conditions. (*A*) Neurons with RFs completely eclipsed by the SPZ. (*B*) Neurons with RFs partially eclipsed by the SPZ and centers within the SPZ. (*C*) Neurons with RFs partially eclipsed by the SPZ and centers outside the SPZ. (*D*) pRF interactions with the rod scotoma. This graph is an accurately scaled visual representation of the normal pRF sizes (measured under photopic conditions) for each visual field map (degrees of visual angle corresponding to the sizes seen here are shown in Fig. S6). Each circle is an accurately scaled visual representation of the average size of pRFs for the eccentricities indicated below it in the map indicated on the left. The eccentricities labeled at the bottom are the centers of the 1° bins used for 10 eccentricity-band ROIs measured for each visual field map. Filled circles represent pRFs in eccentricities where the pRF is both large enough and close enough to the rod scotoma to expect interactions between them. Open circles represent pRFs at eccentricities outside the expected influence of the rod scotoma (see also Fig. S3).

## Results

To compare cortical activity in early visual field maps between photopic (luminance = 140 cd/m$^2$) and scotopic (luminance = 0.003 cd/m$^2$) conditions, we collected fMRI data in four subjects using moving bar stimuli (Fig. 2*F*) after the subjects adapted to each luminance condition (*SI Materials and Methods*). We used population RF (pRF) modeling to estimate the V1, V2, V3, hV4, and VO-1 maps and pRFs (22). A pRF for a particular voxel reflects the central tendency of the sizes (spreads) and centers in visual space preferentially activated by the RFs of the population of neurons within that voxel that are activated by a particular stimulus. An example of the similarity of pRF model fits under photopic and scotopic conditions is presented in Fig. S1. For analysis of the measurements of visual field map activity, shifts of pRF centers, and scaling of pRF sizes, we divided up the eccentricity representation in each map in each hemisphere of each subject into 10 regions of interest (ROIs) spanning 1° of visual angle along the eccentricity gradient from 0° to 10° centered on every 0.5°. Each measurement was drawn from these 10 eccentricity band ROIs for each subject, averaged between hemispheres for each subject, and then, analyzed across subjects between conditions.

We defined the central ROI in each early visual field maps as the maximum region with pRF sizes that are expected to overlap the rod scotoma as measured in the photopic condition (Fig. 1*D*). For example, voxels in V1 with a preferred center of 2.5° of visual angle are estimated by pRF measurements to span ∼1° of visual angle under photopic conditions and thus, would be expected to span visual space approximately from 1.5° to 3.5°, which overlaps the visual span of the rod scotoma. Similarly, voxels in hV4 with a preferred center of 4.5° of visual angle are estimated by photopic pRF measurements to span ∼3.5°; these voxels would, thus, be expected to respond to visual space over a region approximately from 1° to 8°, again partially overlapping the rod scotoma. Therefore, in the following sections, we examine differences between photopic and scotopic conditions in the photopically defined eccentricity representations affected by the rod scotoma (0–3° for V1 and V2, 0–4° for V3, 0–5° for hV4, and 0–6° for VO-1) and contrast those results with representations not affected by the rod scotoma (3–10° for V1 and V2, 4–10° in V3, 5–10° in hV4, and 6–10° in VO-1).

What follows are two multivariate ANOVA comparisons (central and peripheral eccentricities) between photopic and scotopic conditions per measurement type (coherence, preferred eccentricity, and pRF size) (23). Data from the central eccentricities of each map were used to evaluate the effects of the rod scotoma on the neural activity within the SPZ, whereas data from the more peripheral eccentricities were used to evaluate differences between cone and rod inputs. Each measurement was evaluated across subjects to assess group-level results, which is

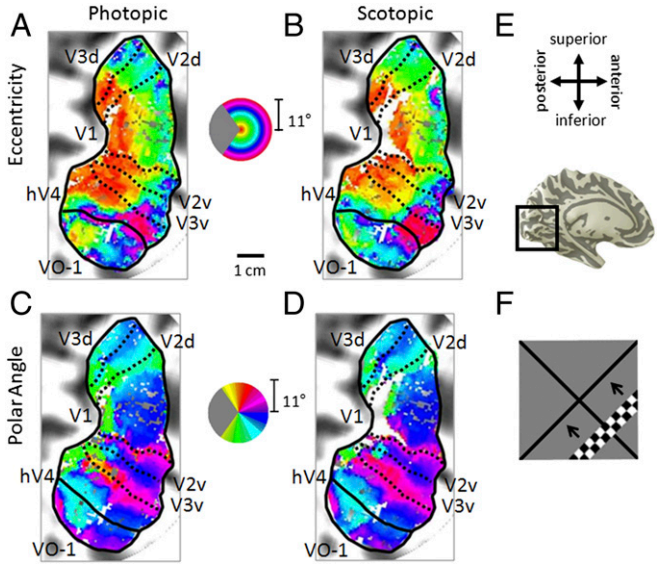


**Fig. 2.** Visual field maps in photopic and scotopic conditions. (*A*–*D*) Pseudocolor overlays on a flattened representation of occipital cortex from the left hemisphere of one subject (S2) represent the position in visual space that produces the strongest response at that cortical location. (*A* and *B*) Eccentricity representations. Color legend represents the visual field from 0° to 10° radius of visual angle. (*C* and *D*) Polar angle representations. Color legend represents the contralateral hemifield. (*A* and *C*) Photopic measurements. (*B* and *D*) Scotopic measurements. Boundaries of visual field maps are depicted with dotted (polar angle boundaries between maps of interest) and solid (eccentricity boundaries and edge of measurement) black lines. Coherence ≥ 0.20. (Scale bar: 1 cm along the flattened cortical surface.) (*E*, *Upper*) Anatomical orientation legend. (*E*, *Lower*) Inflated 3D representation of a medial view of the left hemisphere of subject 2. *Inset* indicates the region near the calcarine sulcus of the occipital lobe, where the maps were measured. (*F*) Moving bar stimulus for visual field map and pRF measurements comprised a set of contrast-reversing checkerboard patterns at eccentricities from 0° to 11° radius. One frame is shown for the bar stimulus sequence. Four bar orientations (0°, 45°, 90°, and 135° from vertical) with two motion directions orthogonal to each orientation were used, producing eight different bar configurations. Additional examples are in Fig. S2.

only possible for such detailed measurements through the presently used functional (not anatomical) localization (24, 25).

**Scotopic and Photopic Visual Field Map Measurements.** Typical pRF measurements of the eccentricity and polar angle representations in V1, V2, V3, hV4, and VO-1 under photopic and scotopic conditions are presented in Fig. 2 for the left hemisphere of one subject (Fig. S2). Note the loss of blood oxygen level-dependent response in the central foveal representation (darkest red voxels drop out of the image in Fig. 2*B*) in the eccentricity representation of V1 under scotopic conditions (Fig. 2*B* and Fig. S2 *B*, *D*, and *F*), consistent with previous findings (6, 7). Interestingly, V2, V3, hV4, and VO-1 did not show a similar loss of signal but rather, a peripheral shift in their central eccentricity representations between photopic and scotopic conditions (red/orange voxels shift to orange/yellow/green in Fig. 2*B* and Fig. S2 *B*, *D*, and *F*). This eccentricity shift represented in the color overlays here is further quantified in graphical form in Fig. 3*B*. It is likely that this shift was produced as neurons with small RFs within this region in each visual field map that did not overlap the rod scotoma edge were silenced, whereas the neurons with larger RFs overlapping the scotoma border are measured as effectively representing a more peripheral position (Fig. S3*B*) (17). The moving bar stimulus at this size (Fig. 2*F*) typically does not produce clear measurements of the polar angle representation within the very central fovea (hence, cyan color in the central photopic polar angle map of V1 in Fig. 2*C* and Fig. S2 *A*, *C*, and *E*) but contrasts with the loss of contralateral responses in this region under scotopic conditions (Fig. 2*D* and Fig. S2 *B*, *D*, and *F*). Outside of this region, the polar angle representations in all visual field maps remained largely unchanged between the two conditions. Because differences in eye movements between conditions could contribute to problems in measuring visual field maps, we confirmed that no significant differences in fixation stability existed between the two conditions (26) (*SI Materials and Methods*, Fig. S4, and Table S1).

**Neural Activity Is Reduced Within the SPZ.** Coherence was measured for voxels in each visual field map across the entire stimulated visual field and compared between scotopic and photopic conditions to assess changes in blood oxygen level-dependent signal caused by the differences in luminance (Fig. 3*A*, *SI Materials and Methods*, and Fig. S5). Across all five maps, photopic coherence was not statistically significantly greater than scotopic coherence in the more peripheral eccentricities (*ps* = 0.078–0.897), which indicates that responses in early visual areas are generally robust under scotopic conditions, despite the drastic drop in luminance and the activation of an entirely different class of photoreceptors between photopic and scotopic conditions (Figs. S4*A* and S5 and Table S2). Within the central eccentricities of each map, where pRFs interact with the rod scotoma, we observed significant decreases in the coherence of V1 ($P = 0.016$), V2 ($P = 0.044$), and V3 ($P = 0.013$) but not hV4 ($P = 0.624$) or VO-1 ($P = 0.465$) (Fig. 3*A*, Fig. S5, and Table S2).

These results indicate that there is a specific drop in neural activity in these visual field maps caused by the silencing of neurons with RFs partially or completely eclipsed by the rod scotoma (Fig. S3). The pattern of results across visual field maps is consistent with the pRF sizes for each of the maps (Fig. 1*D*), such that maps with larger pRFs—hV4 and VO-1, which have proportionally less surface area eclipsed by the rod scotoma—are not

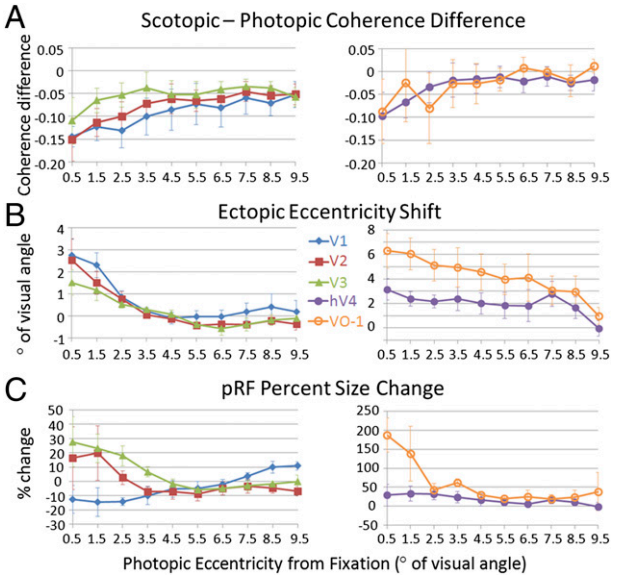


**Fig. 3.** Coherence, eccentricity shifts, and pRF size changes in central and peripheral eccentricities. (*A*) Coherence differences. (*B*) Ectopic eccentricity shifts. Positive numbers indicate shifts of pRF centers outward from the rod scotoma, and negative numbers indicate shifts of pRF centers into the rod scotoma. (*C*) Scotopic pRF size percentage changes. Positive values indicate larger pRF sizes under scotopic conditions, whereas negative values indicate smaller pRF sizes under scotopic conditions. All data are plotted as a function of the photopic eccentricity in degrees of visual angle. The legend indicates line shading and marker shape for each map. Error bars represent SEMs (Figs. S5–S7).

significantly silenced within the central representation. Conversely, maps with smaller pRF sizes—V1, V2, and V3, which are proportionally more eclipsed by the rod scotoma—do undergo significant silencing of neural activity within the central representation (2, 27).

**Voxels with pRFs Overlapping the Rod Scotoma Show an Ectopic Shift in Their pRF Centers.** Preferred eccentricity was measured for voxels in each visual field map across the entire stimulated visual field and compared between scotopic and photopic conditions to assess changes caused by the differences in luminance (Fig. 3*B* and Fig. S6). Across the more peripheral eccentricities of all five maps, there was no significant peripheral shift in pRF locations for scotopic relative to photopic conditions ($ps$ = 0.091–0.740) (Fig. 3*B*, Fig. S6, and Table S2). However, there was a significant shift peripherally from the rod scotoma in scotopic relative to photopic conditions for the central eccentricities of all five maps ($ps$ = 0.023–0.049) (Fig. 3*B*, Fig. S6, and Table S2).

These findings pose a significant problem for fMRI and electrophysiological studies of cortical responses to scotomas reporting ectopic responses from a population of neurons in the SPZ as evidence of reorganization without taking into account effects of short-term adaptation (28–33). Here, we achieved the same results in the SPZ of the rod scotoma with short-term exposure to scotopic conditions. In fMRI measurements, each voxel summarizes the summed activity of hundreds of thousands of neurons, but if a substantial number of those neurons is silenced, because their RF is over the scotoma, the summed RF now only draws from the more active, peripheral individual RFs and shifts more eccentric from the scotoma, which we see here. Similarly, in electrophysiological studies of single neurons, these short-term changes in measurements may arise because of a similar effect at the level of the retinal ganglion cells; the RFs of the neurons in this case each may be drawing from several ganglion cells, some of which are silenced within the scotoma, whereas the more peripheral ganglion cells remain active. Studies of long-term cortical plasticity using any measurement must show that any ectopic responses caused by long-term reorganization are above and beyond the effects of such short-term cortical adaptation (2, 17). Note that fMRI measurements of ectopic responses from long-term reorganization have been successfully shown in the rod scotoma SPZs in rod monochromats (which have a condition that produces congenital, bilateral foveal lesions in the rod-free zone) (7) by comparing these ectopic responses in the rod monochromat subjects with rod scotoma SPZ measurements in control subjects.

**Voxels with pRFs Overlapping the SPZ May Scale pRF Sizes.** pRF sizes were measured for voxels in each visual field map across the entire stimulated visual field and compared between scotopic and photopic conditions to assess changes caused by the differences in luminance (Fig. 3*C* and Fig. S7). The scaling of pRF sizes was evaluated using a measure of the percentage change in pRF sizes between luminance conditions: pRF size percentage change = (scotopic pRF size/photopic pRF size − 1) × 100. Positive values would indicate a larger pRF size under scotopic conditions, whereas negative values would indicate smaller pRF sizes under scotopic conditions. Across the more peripheral eccentricities of all five maps, there was no significant pRF size scaling in scotopic relative to photopic conditions ($ps$ = 0.200–0.628) (Fig. 3*C*, Fig. S7, and Table S2). There also was not a significant difference in pRF size percentage change between photopic and scotopic conditions for V2, V3, or hV4 ($ps$ = 0.131–0.436). However, there was a marginally significant pRF size percentage decrease in the central eccentricities for V1 ($P$ = 0.062) and a significant increase for VO-1 ($P$ = 0.015) (Fig. 3*C*, Fig. S7, and Table S2).

These results indicate that scaling is quite variable among maps because of the rod scotoma; decreasing, not changing, and increasing pRF sizes were all observed. It is possible that these changes reflect differences in attentional modulation from higher-order visual field maps or perhaps, differences in the properties of the individual maps, such as differences in initial pRF sizes or lateral connectivity (2, 17, 18, 34). For the more peripheral eccentricities, these results indicate that there is no observable cortical difference at this measurement level in pRF size between the rod and cone processing pathways.

## Discussion

In summary, the central eccentricities of these visual field maps, with pRFs overlapping the SPZ, generally (*i*) reduced their coherence because of silenced neurons, (*ii*) shifted their pRF centers more eccentric from the rod scotoma, and (*iii*) had variable results regarding scaling of their pRF sizes (increase, decrease, and no change). Each of these measurements was independent of long-term plasticity, which has particularly important implications for the interpretation of studies of cortical reorganization. Although several electrophysiological and fMRI studies propose long-term cortical reorganization as the primary mechanism for silencing, ectopic shifts, and pRF scaling within the SPZ (29, 31–33, 35), we have acquired a similar pRF-level measurement and shown that these responses can arise during short-term cortical adaptation in the representation of pRFs with some overlap with the SPZ.

In contrast, the more peripheral eccentricities of these visual field maps, with pRFs independent of the rod scotoma, (*i*) had no statistically significant reductions in coherence, (*ii*) did not shift their pRF centers, and (*iii*) did not scale their pRF sizes. Although there was no significant reduction in coherence, there tended to be a nonsignificant drop in coherence. Crucially, the drop in coherence observed in the central eccentricities is larger than in the midperiphery. In general, these results act as an ideal within-subject, within-map control, differentiating the effects of the rod scotoma from the luminance drop between photopic and scotopic conditions. Furthermore, these results indicate that retinal differences between rod and cone photoreceptors do not translate to measurable differences at the cortical level of these five visual field maps.

**Comparisons with Studies on the Cortical Effects of Other Retinal Scotomas.** Keys to understanding cortical responses to scotomas are the following questions. Are silencing, ectopic shifts, and RF scaling in cortical SPZs the result of short-term adaptation and thus, the expected immediate response of the visual system to a removal of visual input? Alternatively, do such responses primarily arise over a longer period after more extensive cortical reorganization? Scotomas caused by trauma or disease are challenging for human SPZ studies, because they tend to be permanent, monocular, variable in retinal thicknesses, and difficult to compare across patients because of variability in retinal or cortical location and time of onset. The blind spots, although they are omnipresent, naturally occurring scotomas, are located in the midperiphery, where there is less cortex devoted to visual analysis, and the RFs are larger relative to the fovea (4, 5, 10). Not surprisingly, fMRI studies of the blind spot can only localize a small area of V1 corresponding to the blind spot, which does not make it ideally suited for these questions of ectopic responses and plasticity (36, 37). Artificial, reversible scotomas caused by stabilization of the stimulus on the retina are transient and most effective in the periphery (38), making them difficult to measure in early visual areas with fMRI because of the comparatively slow temporal resolution of fMRI and the relatively smaller amount of cortex devoted to peripheral processing (10, 11, 39, 40).

As a result, many researchers have focused on studying long-term reorganization in early visual cortex in cat and monkey in response to induced binocular retinal lesions, but even these studies have very controversial results (2, 41). Some groups using electrophysiology have reported silencing, ectopic shifts, and pRF scaling from V1 neurons within the SPZ that they use as evidence of cortical reorganization weeks to months after the retinae were lesioned (28–33). However, because these studies typically measure only immediate postlesion and long-term (weeks to months) time points, they cannot differentiate responses in the SPZ caused by short-term adaptation from those arising from long-term reorganization (Fig. S3). The retinal tissue surrounding the experimentally lesioned site takes up to 2 wk to recover normal function after initial swelling from such lesion-inducing procedures as photocoagulation, which prevents accurate measurements immediately after the retinal lesion (27, 28, 42). Furthermore, measurements of short-term adaptation in these cases are inherently confounded by the effects of this retinal stunning that surrounds the true retinal lesion.

In contrast, other groups using electrophysiology and fMRI report no evidence of ectopic responses in the macaque V1 SPZ after weeks of recovery and therefore, no cortical reorganization (2, 27). It is important to note that none of these studies can measure the same neuron at multiple time points, but rather, they must sample from active neurons in similar locations, resulting in potential sampling biases that further complicate their interpretations (2, 27). Similar conflicting measurements have been seen in human patients with bilateral foveal lesions from age-related macular degeneration, with some fMRI studies claiming extensive recovery within the V1 SPZ, whereas again, others showed no evidence for reorganization (7, 18, 35, 43–45).

Thus, the predicted and measured effects on (p)RFs caused by short-term adaptation and long-term reorganization are very difficult to differentiate (Fig. S3). To avoid a potential overestimation of the extent of long-term cortical reorganization and recovery within the SPZ, measurements must be able to determine that long-term reorganization has occurred that is greater than both what can be attributed to short-term adaptation, as described here, and what can be attributed to the recovery of the stunned retinal tissue. Often, one could argue that silencing, shifting, and scaling of (p)RFs in response to a scotoma are short-term adaptations at work but have simply been mistaken for long-term cortical reorganization in many cases. Our goal here was to use measurements of the human rod SPZ to allow for detailed evaluation of immediate human cortical responses to the reversible removal of visual input.

Our data are largely consistent with and extend the recent findings that central retinal lesions caused by age-related macular degeneration and simulated lesions in the central (5° and 7.5° radius) visual field in control subjects show ectopic pRF shifts, silencing, and scaling in V1 caused by cortical short-term adaptation rather than long-term reorganization (17, 18). We note that our data differ in our measurements of a small, marginally significant decrease in pRF size in V1 caused by the rod scotoma, whereas these studies showed an increase in V1 pRF size caused by age-related macular degeneration and artificial scotomas. One possibility for this difference is that our bar stimulus, which spans the central visual field, may have elicited a greater perception of filling in than the expanding ring and rotating wedge stimuli used in the prior studies, leading to alterations in pRF dynamics (46). We have compared such differences in perceptual filling in between these stimulus types in other measurements and do find greater perceptual filling in for the bar stimulus (47). Another factor may be the differences in the sizes of the scotomas; the previously measured scotomas are much larger, on average, than the rod scotoma presently measured. The larger scotoma increases the average pRF size affected by the scotoma because of the well-documented enlargement in pRF size from the representation of central fixation to that of the periphery in visual field maps (22). Interestingly, we do observe increases in pRF sizes caused by the rod scotoma for larger pRFs, which we measured in VO-1, consistent with these previous findings in V1 (Fig. 1*D* shows a model of pRF sizes by map and eccentricity). We do not believe that this difference in V1 pRF sizes arises from the different photoreceptors activated in each study (rods vs. cones). We expect that any such differences in the rod vs. cone visual pathways would be evident across our analysis of the peripheral eccentricities of the visual field (7). However, we see no differences between photopic and scotopic conditions in the relatively more peripheral eccentricities of any of five visual field maps.

**Rod Pathways in Cortex.** Comparatively few studies have examined the contributions of the rod system to cortical activity. Our measurements support the studies of scotopic psychophysics and retinal circuitry, which suggest that most, if not all, retinal ganglion cell types—and thus, the cone pathways—contribute to scotopic vision (13, 14, 48). Outside of the region of interactions with the rod scotoma, we do not measure any differences in visual field map organization or pRF properties across our measurements out to 10° of visual angle between photopic and scotopic conditions, suggesting that these regions in these visual field maps receive similar cone and rod inputs, at least for this level of processing.

With measurements of cortical activation under scotopic vision, Hadjikhani and Tootell (6) also showed similar peripheral responses between photopic and scotopic conditions in V1, V2, V3, and what they measured as V8 (analogous to our hV4 and VO-1) (39), comparable with our findings. However, Hadjikhani and Tootell (6) observed a significant lack of activity in the central representations of their four maps, which is in contrast to our findings of shifts of the central representations to more parafoveal regions in all five maps. We do observe significant decreases of activity, which indicate that many neurons in pRFs overlapping the rod scotoma have reduced activity or are silenced. These differences may have arisen from variations in (*i*) measurement methodology (traveling wave vs. pRF modeling), (*ii*) signal-to-noise ratios, and (*iii*) effects arising from the stimulus types, such as perceptual filling in. Our moving bar stimulus, for example, likely produced a greater effect of filling in, which might be reflected in top-down influences producing activity in foveal V2, V3, hV4, and VO-1 (19, 47). Along these lines, a recent study by Williams et al. (19) showed that feedback from higher cortical areas can produce differential effects in the fovea vs. the periphery of early visual cortex. Specifically, object stimuli presented in the periphery produced responses in foveal retinotopic cortex but not peripheral retinotopic cortex. It is possible that a similar feedback mechanism contributes to the coherence changes, ectopic shifts, and pRF size changes measured here along the scotoma border.

Additionally, Hadjikhani and Tootell (6) observed no activation of the region of hV4 and VO-1 (V8) under scotopic conditions throughout their entire measured visual field, concluding that those maps were cone-only color-processing maps. We observe significant activation of both hV4 and VO-1 when only rods are active, indicating that, although these maps may be involved in color processing, they are not cone-exclusive. From our data, it seems that rod signals are passed through all maps in the early stages of the visual system. There seems to be no differences in any of our measurements of the peripheral eccentricities, indicating that the maps handle rod signals very similarly to cone signals.

Finally, we note that our measurements average across all polar angles within each eccentricity band. Interestingly, there is growing evidence for perceptual and neural asymmetries between the dorsal and ventral visual fields, with improved motion, global processing, and coordinate spatial judgments in the lower

visual field and improved visual search, local processing, and categorical judgments in the upper visual field, especially for the left visual field (49–53). Such variations would not be apparent in our measurements based on eccentricity from fixation, which grouped the polar angles. Although such differences would be unlikely to have an effect on our results here, it may be of interest to future studies to investigate potential differences between these quarter-field representations as well as between hemispheres.

## Conclusions

The use of the rod scotoma provides an excellent, reversible, accessible approach for investigating the short-term responses to scotomas as well as the cortical differences between rod and cone inputs, which we describe here. Claims of long-term cortical recovery in response to retinal scotomas must take into account these rapid cortical adjustments as well as retinal recovery from stunning postlesion and the resulting return to normal function at the edge of the SPZ before being able to conclusively attribute these cortical responses to long-term reorganization. Additionally, rod and cone contributions to V1, V2, V3, hV4, and VO-1 appear quite similar when unaffected by the rod scotoma in peripheral eccentricities, which indicates that cone and rod inputs are treated very similarly at the cortical level.

## Materials and Methods

**Subjects.** Four subjects (two females) ages 24–36 years old participated in this study. All subjects had normal or corrected-to-normal visual acuity. The experimental protocol was approved by the Institutional Review Board at University of California, Irvine, and informed consent was obtained from all subjects.

**Experimental Design.** Each subject underwent two fMRI scan sessions, which involved collecting 1 T1-weighted anatomical volume, 2 T1-weighted in-plane anatomical scans, and 16 functional visual field mapping scans (moving bar stimulus) under both photopic (luminance = 140 cd/m$^2$) and scotopic (luminance = 0.003 cd/m$^2$) conditions (8 scans per condition). Our data analysis used pRF modeling to estimate the visual field map organization and pRF sizes and centers (22) (*SI Materials and Methods*).


1. Dreher B, Burke W, Calford MB (2001) Cortical plasticity revealed by circumscribed retinal lesions or artificial scotomas. *Prog Brain Res* 134:217–246.
2. Wandell BA, Smirnakis SM (2009) Plasticity and stability of visual field maps in adult primary visual cortex. *Nat Rev Neurosci* 10(12):873–884.
3. Roorda A, Williams DR (1999) The arrangement of the three cone classes in the living human eye. *Nature* 397(6719):520–522.
4. Curcio CA, Allen KA (1990) Topography of ganglion cells in human retina. *J Comp Neurol* 300(1):5–25.
5. Curcio CA, Sloan KR, Kalina RE, Hendrickson AE (1990) Human photoreceptor topography. *J Comp Neurol* 292(4):497–523.
6. Hadjikhani N, Tootell RB (2000) Projection of rods and cones within human visual cortex. *Hum Brain Mapp* 9(1):55–63.
7. Baseler HA, et al. (2002) Reorganization of human cortical maps caused by inherited photoreceptor abnormalities. *Nat Neurosci* 5(4):364–370.
8. Duffy KR, Hubel DH (2007) Receptive field properties of neurons in the primary visual cortex under photopic and scotopic lighting conditions. *Vision Res* 47(19):2569–2574.
9. Hubel DH, Howe PD, Duffy AM, Hernández A (2009) Scotopic foveal afterimages. *Perception* 38(2):313–316.
10. Dougherty RF, et al. (2003) Visual field representations and locations of visual areas V1/2/3 in human visual cortex. *J Vis* 3(10):586–598.
11. Wandell BA, Dumoulin SO, Brewer AA (2007) Visual field maps in human cortex. *Neuron* 56(2):366–383.
12. Schira MM, Tyler CW, Breakspear M, Spehar B (2009) The foveal confluence in human visual cortex. *J Neurosci* 29(28):9050–9058.
13. Field GD, et al. (2009) High-sensitivity rod photoreceptor input to the blue-yellow color opponent pathway in macaque retina. *Nat Neurosci* 12(9):1159–1164.
14. Stockman A, Candler T, Sharpe LT (2010) Human scotopic sensitivity is regulated postreceptorally by changing the speed of the scotopic response. *J Vis* 10(2):12.1–12.19.
15. Xing J, Heeger DJ (2000) Center-surround interactions in foveal and peripheral vision. *Vision Res* 40(22):3065–3072.
16. Xing J, Heeger DJ (2001) Measurement and modeling of center-surround suppression and enhancement. *Vision Res* 41(5):571–583.
17. Haak KV, Cornelissen FW, Morland AB (2012) Population receptive field dynamics in human visual cortex. *PLoS ONE* 7(5):e37686.
18. Baseler HA, et al. (2011) Large-scale remapping of visual cortex is absent in adult humans with macular degeneration. *Nat Neurosci* 14(5):649–655.
19. Williams MA, et al. (2008) Feedback of visual object information to foveal retinotopic cortex. *Nat Neurosci* 11(12):1439–1445.
20. Sirotin YB, Das A (2009) Anticipatory haemodynamic signals in sensory cortex not predicted by local neuronal activity. *Nature* 457(7228):475–479.
21. Lehky SR, Sereno AB (2011) Population coding of visual space: Modeling. *Front Comput Neurosci* 4:155.
22. Dumoulin SO, Wandell BA (2008) Population receptive field estimates in human visual cortex. *Neuroimage* 39(2):647–660.
23. Brewer AA, Barton B (2014) Visual cortex in aging and Alzheimer's disease: Changes in visual field maps and population receptive fields. *Front Psychol* 5:74.
24. Brewer AA, Barton B (2012) Visual field map organization in human visual cortex. *Visual Cortex—Current Status and Perspectives*, eds Molotchnikoff S, Rouat J (InTech, New York), pp 29–60.
25. Brewer AA, Barton B (2014) Developmental plasticity: FMRI investigations into human visual cortex. *Advanced Brain Neuroimaging Topics in Health and Disease—Methods and Applications*, eds apageorgiou DT, Smirnakis SM, Christopoulos G (InTech, New York), pp 305–334.
26. Beauchamp MS (2003) Detection of eye movements from fMRI data. *Magn Reson Med* 49(2):376–380.
27. Smirnakis SM, et al. (2005) Lack of long-term cortical reorganization after macaque retinal lesions. *Nature* 435(7040):300–307.
28. Giannikopoulos DV, Eysel UT (2006) Dynamics and specificity of cortical map reorganization after retinal lesions. *Proc Natl Acad Sci USA* 103(28):10805–10810.
29. Calford MB, et al. (2005) Neuroscience: Rewiring the adult brain. *Nature* 438(7065):E3.
30. Darian-Smith C, Gilbert CD (1994) Axonal sprouting accompanies functional reorganization in adult cat striate cortex. *Nature* 368(6473):737–740.
31. Gilbert CD, Wiesel TN (1992) Receptive field dynamics in adult primary visual cortex. *Nature* 356(6365):150–152.
32. Heinen SJ, Skavenski AA (1991) Recovery of visual responses in foveal V1 neurons following bilateral foveal lesions in adult monkey. *Exp Brain Res* 83(3):670–674.
33. Kaas JH (1991) Plasticity of sensory and motor maps in adult mammals. *Annu Rev Neurosci* 14:137–167.
34. Ress D, Backus BT, Heeger DJ (2000) Activity in primary visual cortex predicts performance in a visual detection task. *Nat Neurosci* 3(9):940–945.
35. Baker CI, Peli E, Knouf N, Kanwisher NG (2005) Reorganization of visual processing in macular degeneration. *J Neurosci* 25(3):614–618.
36. Awater H, Kerlin JR, Evans KK, Tong F (2005) Cortical representation of space around the blind spot. *J Neurophysiol* 94(5):3314–3324.
37. Dilks DD, Baker CI, Liu Y, Kanwisher N (2009) "Referred visual sensations": Rapid perceptual elongation after visual cortical deprivation. *J Neurosci* 29(28):8960–8964.
38. Ramachandran VS (1992) Filling in the blind spot. *Nature* 356(6365):115.
39. Brewer AA, Liu J, Wade AR, Wandell BA (2005) Visual field maps and stimulus selectivity in human ventral occipital cortex. *Nat Neurosci* 8(8):1102–1109.
40. Wandell BA, Brewer AA, Dougherty RF (2005) Visual field map clusters in human cortex. *Philos Trans R Soc Lond B Biol Sci* 360(1456):693–707.
41. Hooks BM, Chen C (2007) Critical periods in the visual system: Changing views for a model of experience-dependent plasticity. *Neuron* 56(2):312–326.
42. DeAngelis GC, Anzai A, Ohzawa I, Freeman RD (1995) Receptive field structure in the visual cortex: Does selective stimulation induce plasticity? *Proc Natl Acad Sci USA* 92(21):9682–9686.
43. Liu T, et al. (2010) Incomplete cortical reorganization in macular degeneration. *Invest Ophthalmol Vis Sci* 51(12):6826–6834.
44. Masuda Y, Dumoulin SO, Nakadomari S, Wandell BA (2008) V1 projection zone signals in human macular degeneration depend on task, not stimulus. *Cereb Cortex* 18(11):2483–2493.
45. Sunness JS, Liu T, Yantis S (2004) Retinotopic mapping of the visual cortex using functional magnetic resonance imaging in a patient with central scotomas from atrophic macular degeneration. *Ophthalmology* 111(8):1595–1598.
46. Komatsu H (2006) The neural mechanisms of perceptual filling-in. *Nat Rev Neurosci* 7(3):220–231.
47. Barton B, Brewer AA (2011) FMRI of the rod cotoma: Filling-in, rod pathway projections, and insights into plasticity. *Journal of Vision* 11(15):9.
48. Buck SL, Knight RF, Bechtold J (2000) Opponent-color models and the influence of rod signals on the loci of unique hues. *Vision Res* 40(24):3333–3344.
49. Lee B, Kaneoke Y, Kakigi R, Sakai Y (2009) Human brain response to visual stimulus between lower/upper visual fields and cerebral hemispheres. *Int J Psychophysiol* 74(2):81–87.
50. Thomas NA, Elias LJ (2011) Upper and lower visual field differences in perceptual asymmetries. *Brain Res* 1387:108–115.
51. Danckert J, Goodale MA (2001) Superior performance for visually guided pointing in the lower visual field. *Exp Brain Res* 137(3-4):303–308.
52. Skrandies W (1987) The upper and lower visual field of man: Electrophysiological and functional differences. *Prog Sens Physiol* 8:1–93.
53. Previc FH (1990) Functional specialization in the lower and upper visual fields in humans: Its ecological origins and neurophysiological implications. *Behav Brain Sci* 13:519–575.